Optimisation of a novel trailing edge concept for a high lift device

Jason D.M. Botha[*1], Laurent Dala[2a] and S. Schaber[3b]

[1]*School of Mechanical Industrial and Aeronautical Engineering, University of the Witwatersrand, Private Bag 3, Wits 2050, South Africa*
[2]*CSIR, DPSS: Aeronautics Systems, PO Box 395, Pretoria 0001, South Africa*
[3]*Airbus Operations GmbH, AIRBUS-ALLEE 1, D-28199 Bremen, Germany*

Abstract.   This study aimed to observe the effect of a novel concept (referred to as the flap extension) implemented on the leading edge of the flap of a three element high lift device. The high lift device, consisting of a flap, main element and slat is designed around an Airbus research profile for sufficient take off and landing performance of a large commercial aircraft. The concept is realised on the profile and numerically optimised to achieve an optimum geometry. Two different optimisation approaches based on Genetic Algorithm optimisations are used: a zero order approach which makes simplifying assumptions to achieve an optimised solution: as well as a direct approach which employs an optimisation in ANSYS DesignXplorer using RANS calculations. Both methods converge to different optimised solutions due to simplifying assumptions. The solution to the zero order optimisation showed a decreased stall angle and decreased maximum lift coefficient against angle of attack due to early stall onset at the flap. The DesignXplorer optimised solution matched that of the baseline solution very closely. The concept was seen to increase lift locally at the flap for both optimisation methods.

Keywords: aerodynamic design; high lift; single slotted flap; optimization; aeroacoustics; CFD

1. Introduction

Single slotted high lift devices, in their current form, are not the most efficient devices for their use. Currently they provide a *good enough* solution to their requirements for take off and landing but are seen as a roadblock to further aerodynamic enhancement of high lift device design.

Rudolph (1996) discusses a number of roadblocks for single slotted flaps. He explains that there are two major obstacles; the first is that a single slotted flap produces a lower maximum lift coefficient than that of flaps with additional slots, and, that this may be insufficient for landing. Secondly, the single slotted flap could allow for unnecessarily high airplane attitude at landing which is unfavourable. He adds that a single slotted flap should not provide problems during take

---

∗Corresponding author, Ph.D. Student, E-mail: jasonbot@gmail.com
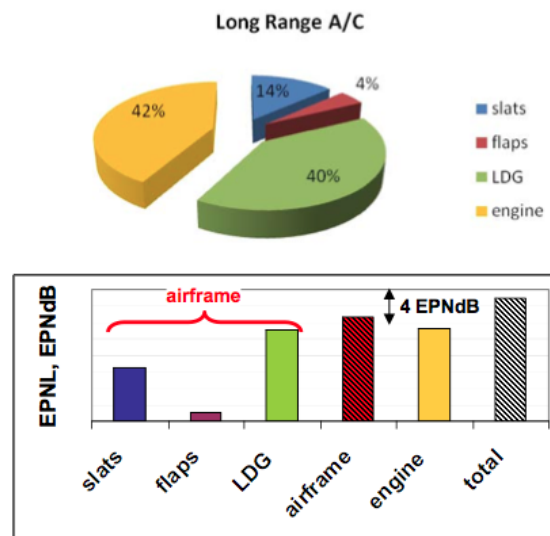[a]Ph.D.
[b]Dr.-Ing

Fig. 1 Aircraft noise levels by component during approach (Dobrzynski 2008)

off.

Meredith (1993) lists the following trade-off factors for a generic large twin engine aircraft in order to illustrate the need for high lift system improvements:

• An increase in lift coefficient of 0.10 at constant angle of attack results in a reduction in approach attitude of one degree. This results in a shortening of landing gear due to lower ground clearance requirements and thus a weight saving of 635 kg.

• A 1.5% increase in maximum lift coefficient is equivalent to a 2994 kg increase in payload at a fixed approach speed.

• A 1% increase in take off L/D is equivalent to a 1270 kg increase in payload or a 150 nm increase in range. Modern aircraft are aiming to become quieter for both passengers, as well as those living near airports, as noise is both a nuisance and a health risk. In the past few decades there has been a shift in focus within aircraft design and operations, which has aimed to determine aircraft noise sources and find ways in which to minimise or alleviate their effects.

Fig. 1 shows the EPN (Effective Perceived Noise) generated by a generic long range commercial aircraft (Herr 2012). Dobrzynski (2008) explains that for the same air speed, an aircraft in the landing configuration will produce 10 dB more noise due to deployment of high lift systems. It is broadly perceived that an increase of 10 dB is perceived to be a doubling of loudness. Zhang (2010), Casalino *et al.* (2008) identify primary noise sources within high lift devices- slats (including the spoiler cove), flap side edges, slat tracks and flap tracks and the trailing edges of all elements.

The European Framework FP-7 highlights a European Vision for the year 2020 with regards to development within numerous research disciplines, one of these being transport, and, on a sub-level, air transport.

According to this European Vision for 2020, ACARE (Advisory Council for Aeronautics Science in Europe) has highlighted some research challenges for the 2020 vision (Busquin 2001). Related to high lift systems (amongst other aircraft subsystems) are the following:

• Drag reduction through conventional and novel shapes.

- Noise Reduction:
  ◦ Reduction in perceived noise to one half of current average levels (10 dB).
- Emission Reduction:
  ◦ 50% cut in CO_2 emissions per passenger kilometre (which means a 50% cut in fuel consumption in the new aircraft of 2020) and an 80% cut in nitrogen oxide emissions.
- Environmentally friendly production, maintenance and disposal

A GA (Genetic Algorithm) is a search heuristic optimisation process based on the biological model of genes and how they reproduce. It mimics the process of natural selection to evolve a solution to a global minimum by means of modifying input populations over a series of generations. The GA provides input to a 'black box' solver and receives the output from the solver as the objective function. The GA recreates a fitness landscape of $n \times m$ dimensions where n is the number of design variables (input to the solver) and m, the number of objectives (output of the solver). Each population tends closer to the global minimum and when the distance between populations falls below the convergence criteria the solution is produced.

Applications of the process are widespread and have been successful in finding optimum solutions for aerospace applications. There have been a number cases where GA's have been used to numerically optimise high lift devices. Many optimisations have been directed towards finding optimum flap and slat settings for the gap and overlap parameters (Chen *et al*. 2012, Soulat *et al*. 2012, Taylor *et al.* 2013). Shape optimisations have also seen some success (Wild, 2008). These optimisations aim to produce optimum shapes for the slat and flap in order to increase high lift performance.

Bizzarrini *et al*. (2011) performs an airfoil multi disciplinary optimisation for a power generating wind turbine which couples an airfoil flow solver with a noise prediction tool (NAFnoise). The result is a series of airfoils which exhibit a decrease in A-weighted noise of up to just over 1 dB and an increase in L/D of up to 14. Kuo and Sarigul-Klijn (2012) studies the effect of using micro tabs to minimise noise. Overall a decrease in noise of 2.4dB is achieved.

As a result of these observations new high lift concepts need to be examined which are able to increase aerodynamic performance and reduce noise. The concept examined in this study aims to reduce aerodynamically generated noise and increase the maximum lift coefficient of the Airbus TC12 profile in high lift, take off, configuration. Optimisation of the concept is performed numerically using a Genetic Algorithm to find an optimum geometry, which fulfills the design criteria.

2. Novel concept

The approach to optimise the TC12 profile for landing configuration is to implement a novel concept at the leading edge of the flap. Fig. 2 shows the TC12 profile in landing configuration, as well as the region in which the optimisation will occur. The novel concept to be implemented is a 'betz flap' (see Fig. 3) (ENSICA, 1980). The flap extension will be stored within the flap of the TC12 profile during cruise and will extend out of the leading edge of the flap during landing. The concept, thus referred to as the *'flap extension'*, will act similar to an upper surface krueger flap (Fullmer 1947). Increases in lift should be achieved because of an increase in the camber and area of the TC12 flap, thus increasing local lift in this vicinity. An increase in lift at the flap should increase circulation around the entire high lift device. This should not only locally increase flap lift but also increase lift upstream at the main element and the slat thus improving aerodynamic
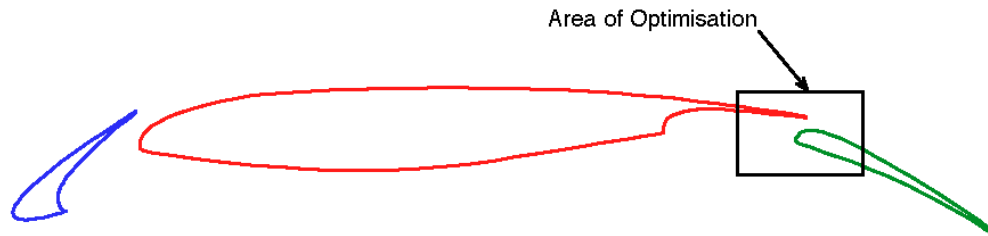
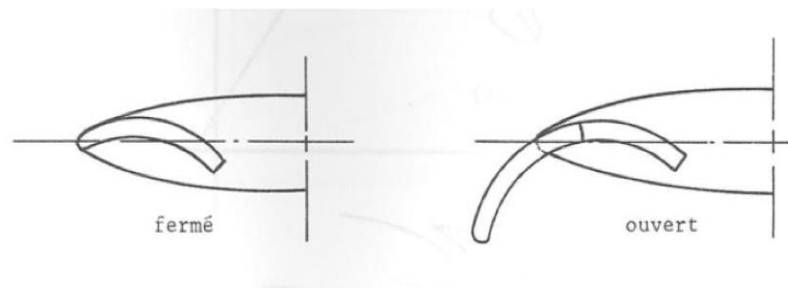Fig. 2 Optimisation region of TC12 airfoil in high lift configuration

Fig. 3 Betz flap (ENSICA 1980)

performance of the entire system.

The flap extension should also have an effect on the recirculation region within the spoiler cove. This should bring stability to the shear layer of fluid flow that borders the recirculation region due to a Coanda effect from the geometric impingement of the concept. Stability of the unsteady pressure fluctuations should minimise noise produced in this vicinity.

3. Zero order optimisation method

The first optimisation procedure selected is a 'zero order' optimisation approach. This process involves optimising the flap of the TC12 profile in isolation (avoiding any effects of the slat and main element of the high lift system). XFOIL is used within a Genetic Algorithm to optimise the flap of the TC12 high lift profile in isolation.

3.1 Optimisation routine

The optimisation is performed entirely within MATLAB. Fig. 4 shows the system diagram of the optimisation. In the diagram *GA* is the MATLAB GA which handles the optimisation procedure, *Geom* is the Geometry Function which creates new geometries, *XFoil* is the program XFOIL[1] (herein referred to as the Aerodynamic Solver) which is used to analyse the geometries

---

[1]An interactive panel code used for analysing subsonic airfoils (Drela 2007)

1. Is geometry valid?
2. Has XFoil provided sufficient data?
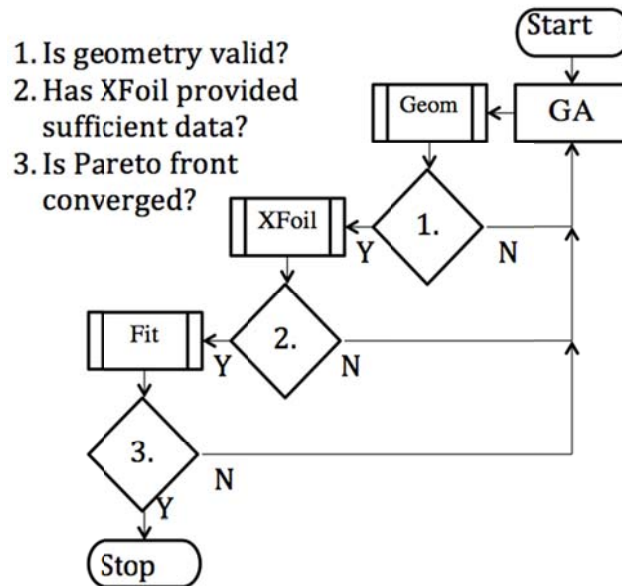3. Is Pareto front converged?

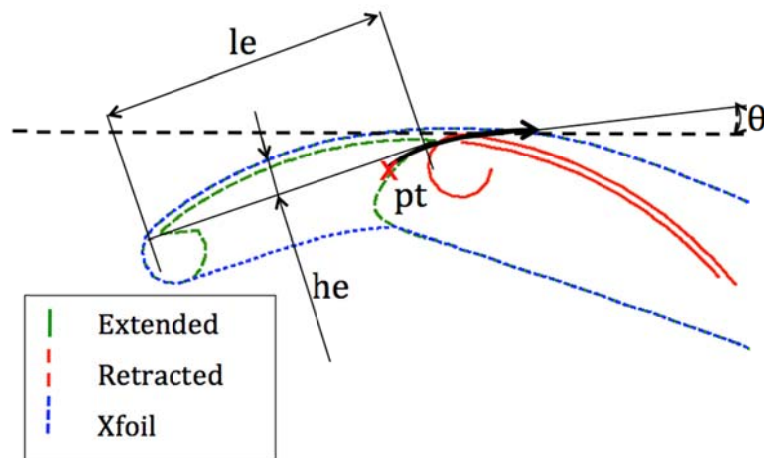

Fig. 4 System diagram of the optimisation routine

Fig. 5 Geometry of solution of zero order flap optimisation

and *Fit* is the multi-objective Objective Function used to determine the feasibility of analysed solutions. The solutions are fed back into the MATLAB Genetic Algorithm where new populations are created and solutions trends monitored. Upon convergence the GA stops and the set of most optimised solutions is provided.

3.2 Geometry function

The geometry function receives the four design variables as input and outputs a geometry. This geometry is checked for any errors and, if successful, it is passed to the aerodynamic solver. If
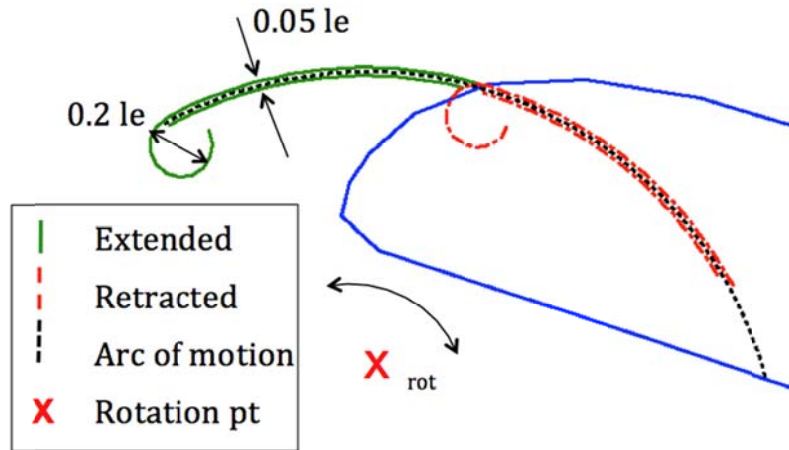
Fig. 6 Constrained optimisation variables

unsuccessful, the aerodynamic solver and objective function are avoided and a very large number is returned to the GA.

Fig. 5 shows the function input variables as characterised by the dimension lines on the figure. Fig. 5 also shows a sample output geometry characterised in extended position by the green dotted line and retracted position by the red solid

3.2.1 Constraints

The kinematic design requirement for the retracted position of the flap extension is shown in Fig. 6 as the red dotted line, the extension and retraction of the concept follows a circular arc of motion. Any concepts generated by the geometry tool that are not able to fulfill the kinematic constraints are automatically rejected by means of a large penalty value output to the GA. The implicit constraints are hardcoded into the geometry tool and are based on the NACA Krueger flap geometry (Fullmer 1947).

3.3 Aerodynamic solver

XFOIL is used to solve the aerodynamic solution of each new configuration generated by the geometry function. XFOIL cannot solve airfoils where there are sharp changes in continuity (high panel angles). Thus, the geometries sent to the solver are splined (the splined region is seen in Fig. 5 as the blue dotted lines) to provide a continuous geometry and better convergence. Eq. (5) represents the input variables for optimisation. a MATLAB function generates a run file for XFOIL which smooths the airfoil geometry within XFOIL, sets XFOIL to run the simulation at a Reynolds number of 2.95 million, runs the simulation at a series of angles of attack and writes the data to a file. Once XFOIL is finished running, a MATLAB function post processes the data and outputs the results to the GA.

The problem statement is to minimise the objective function using real numbers as input (Eq. (2)). Eqs. (2) to (4) are the three objective functions to be solved for, reasoned for selection as follows:

• Maximum lift is a problem for current single slotted flap systems as per Rudolph (1996).

• Lift drag ratios are a good figure of merit when incorporating drag into the objective function. The ratio is a key component in measuring total range of an aircraft. There are also increased benefits of higher L/D for aircraft (Meredith 1993).

• Higher stall angles lead to more protection of the high lift system near stall. Higher stall angles lead to higher maximum lift coefficients.

$$\min(\mathbf{F}_{obj}(\mathbf{x})), (\mathbf{x} \in R) \tag{1}$$

$$\mathbf{F}_{obj,1}(\mathbf{x}) = -C_{L_{\max}} \tag{2}$$

$$\mathbf{F}_{obj,2}(\mathbf{x}) = -\frac{L}{D}_{\max} \tag{3}$$

$$\mathbf{F}_{obj,3}(\mathbf{x}) = \alpha_{stall} \tag{4}$$

$$\mathbf{x} = \begin{Bmatrix} he \\ le \\ al \\ pt \end{Bmatrix} \tag{5}$$

3.4 Convergence

The optimisation converged after the average distance between populations residual dropped below 0.0001. This occurred after 106 generations with a total of 6 418 function evaluations. On a Core 2 Duo machine with 8 Gb RAM- this equated to about three days of processing time. The pareto front of the converged solution is seen in Fig. 7. This is a multi-dimensional figure which represents the objective function values of the optimised solution. The final solution (Fig. 5 shows the geometry of the optimised solution) is selected from the central region of this figure to provide an acceptable trade off of requirements.

4. 2D CFD optimisation method

The second approach to optimise the TC12 profile for landing configuration is performed using ANSYS Workbench which has a number of built in optimisation tools. The optimisation tool used is the ANSYS DesignXplorer MOGA (Multi Objective Genetic Algorithm) tool.

4.1 Optimisation routine

Fig. 8 shows a system diagram for the ANSYS Workbench Direct Optimisation. In the diagram *MOGA* is the optimisation tool, *Geom* is the geometry creation tool, *Mesh* is the Ansys Mesher and *Fluent* is ANSYS Fluent the aerodynamic solver. The modules pass information along to each subsequent module in serial.
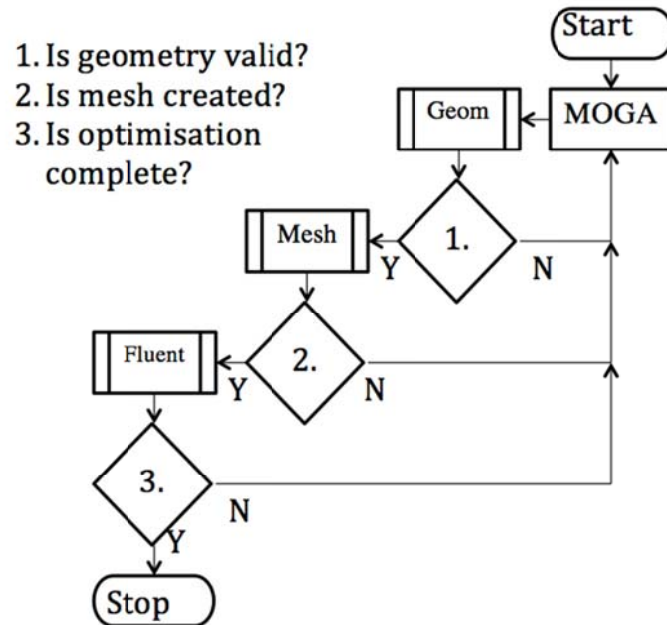
Fig. 8 System diagram of MOGA optimisation in ansys DesignXplorer

4.2 Objective function

The objective function used for the DesignXplorer optimisation was the same function suggested by Brezillon *et al*. (2008) citing better success than merely implementing a lift to drag ratio figure of merit. Eq. (6) states the problem- a maximisation of the objective function. Equation (7) states the objective function, in this instance the climb index. The inclusion of the value *0.00000001* is a workaround used to prevent division by zero because the initial state of the solution is for each point to be zero. Eq. (8) states the input variables to the problem.

$$\max(\mathbf{F}_{obj}(\mathbf{x})),(\mathbf{x} \in R) \tag{6}$$

$$\mathbf{F}_{obj}(\mathbf{x}) = \frac{C_L^3}{C_D^2 + 0.00000001} \tag{7}$$

$$\mathbf{x} = \begin{Bmatrix} le \\ he \\ th \\ \theta \\ ca \end{Bmatrix} \tag{8}$$
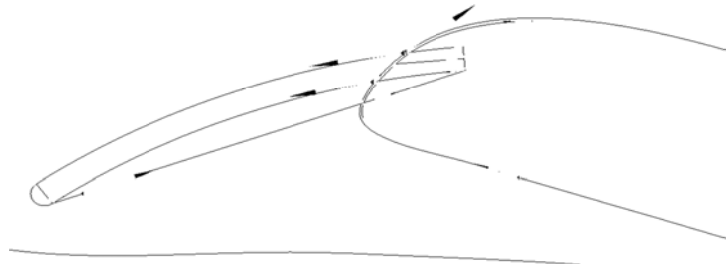
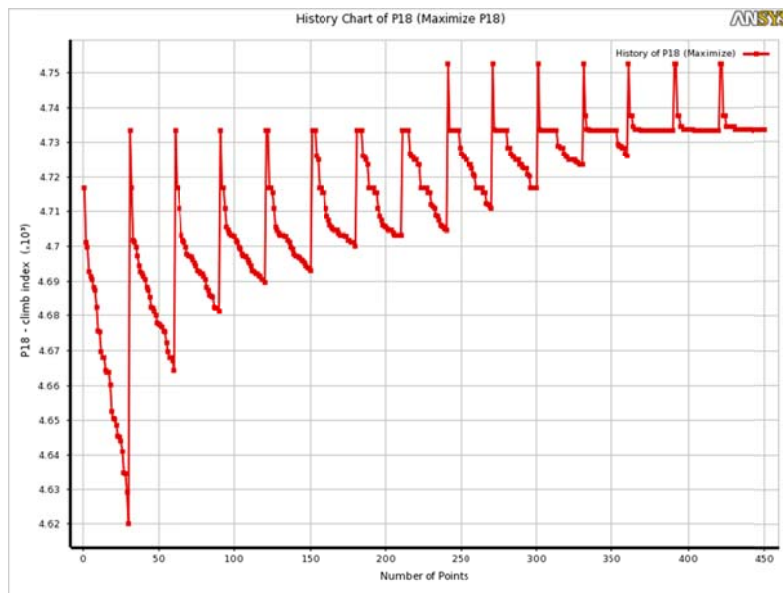Fig. 9 Geometry of DesignXplorer MOGA optimised solution

Fig. 10 Convergence history of DesignXplorer MOGA optimisation of TC12 profile (climb index vs. design point)

4.3 Geometry tool

ANSYS Workbench is used to automatically generate new configurations based on the five input variables to the problem. ANSYS DesignModeler is set up to produce unique geometries similar to Fig. 9. For this optimisation method the leading edge ball, as used in the previous method, was excluded. Also, by using DesignModeler, there was no way to enforce the kinematic constraint required.

4.4 Meshing tool

In order to perform the optimisation quickly each configuration needs to be meshed automatically. A mesh method is set up in ANSYS Mesher, which is applied to each new

geometry. The mesh method needed to be flexible enough to provide acceptable meshes for a range of configurations. After the mesh method was tested manually it was seen to provide acceptable meshes over a range of configurations.

4.5 Convergence

The final solution given by the DesignModeler optimisation is limited by available computation time. The optimisation was set to perform 15 optimisation iterations with 30 samples per iteration. The initial sample set was set to 80 points. The total number of design points was 457 of which 61 of those failed due to impossible geometries being generated by the parametrised geometry creation tool.

Fig. 10 shows the convergence history of the optimisation tool. This plots the objective function against the number of points per optimisation. Each spike and subsequent drop of the objective function represents a single generation. After roughly 200 function evaluations the function maximum value jumps to a new steady value, it is impossible to say (without additional function evaluations) whether or not the function would converge to this given point or to a new more optimum point.

5. Optimisation solutions

The optimised solution selected for the zero order optimisation was successful in increasing aerodynamic performance of the flap in isolation. The flap in isolation yields a 16.7 % increase in stall angle, 11.4 % increase in maximum lift coefficient and a 13.3% percent increase in maximum lift to drag ratio against angle of attack. ANSYS Fluent was used to look at the results of the optimised concept implemented into the full high lift system. Simulations were performed at Mach
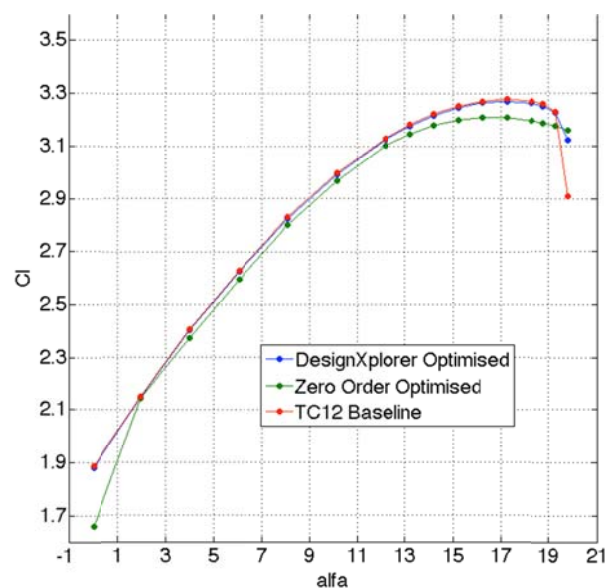

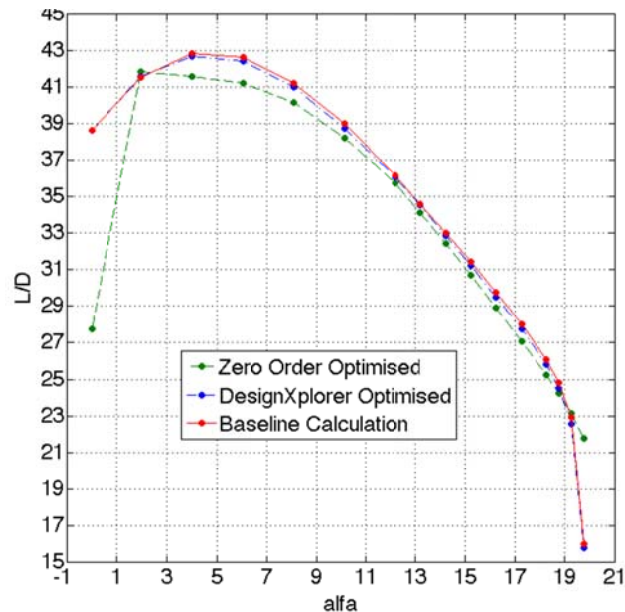Fig. 11 Lift coefficient against angle of attack of optimised results compared to the baseline

Fig. 12 Lift to drag ratio against angle of attack of optimised results compared to the baseline

0.2 and at a Reynolds number of 2.95 million to compare to wind tunnel test data from Airbus. The optimised concept produces less lift than the baseline solution for all angles of attack (Fig. 11). Premature stall is caused by increased flap camber providing early onset of separation at the trailing edge when the angle of attack is increased past 12 degrees. The lift to drag ratio against angle of attack also shows slightly decreased performance (Fig. 12). The leading edge ball is seen as a high drag area. This change in performance is quantified as a decrease of maximum lift of 2.1% and a decrease in stall angle of 5.9%.

The DesignXplorer MOGA optimisation tool achieved a considerably different solution to that of the zero order optimised solution. The optimisation may not have fully converged and the time to final convergence cannot be estimated but the solution still performs better than that of the zero order optimisation method. Lift against angle of attack (Fig. 11) more closely matches that of the baseline TC12 profile. The stall angle is the same as the baseline and maximum lift is decreased by 0.244% (negligible). Drag and lift to drag ratio (Fig. 12) is marginally increased with increasing angle of attack. At an angle of 8.09 degrees drag is increased by 0.3644%.

Fluid flow from the pressure side of the main element airfoil, has the tendency to be attracted to the geometry of the flap extension due to the Coanda effect. The flow attracted to the flap extension has to accelerate along the curved surface, causing a low pressure suction (lifting) region along the flap extension. This suction reduces the recirculation region within the spoiler cove causing a decrease in pressure with span at the trailing edge of the main element (Fig. 13). The data in the figure has been shifted along the *x*-axis for clarity.

6. Aeroacoustic investigations

Acoustic simulations using the transient DES turbulence model are performed on the TC12
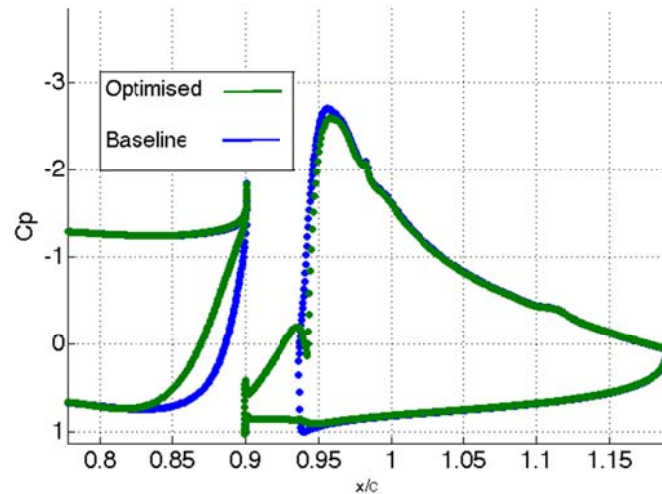
Fig. 13 Pressure coefficient along span of DesignXplorer optimised results compared to the baseline
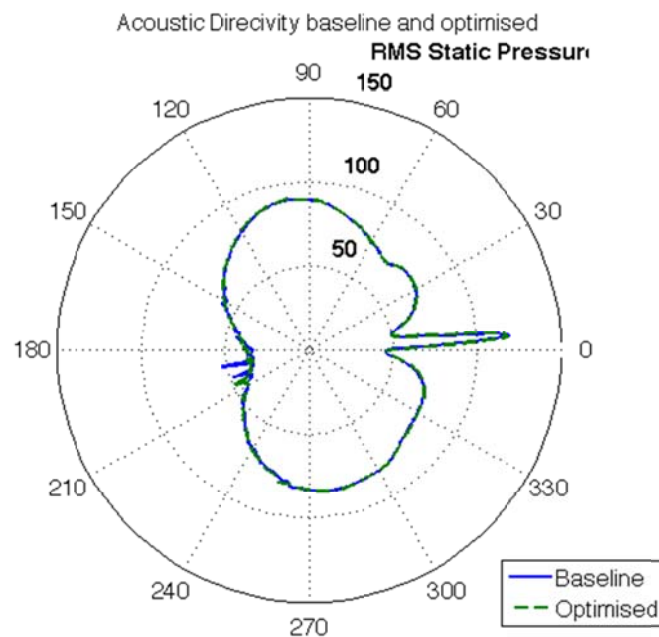

Fig. 14 Directivity of sound for the optimised solution against the baseline at 8.09 degrees angle of attack

profile in high lift configuration as well as on the DesignXplorer optimised solution. The mesh used for calculations is the same as the one used for validation data.

The DES turbulence model is a RANS/LES hybrid model, which employs RANS turbulence formulations near walls and LES formulations away from walls where turbulent length scales are greater and less computationally expensive to simulate. Acoustic calculations are done using the Ffowcs-Williams Hawkings analogy (Ffowcs-Williams and Hawking, 1969) solver built into ANSYS Fluent. 6 000 timesteps are used to reach a sufficiently converged transient simulation
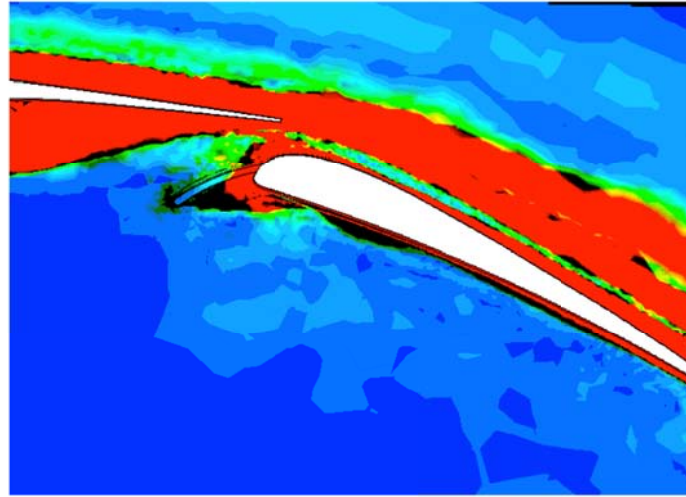
Fig. 15 Vorticity between 0 - 1 000 comparing the baseline configuration and the DesignXplorer optimised solution
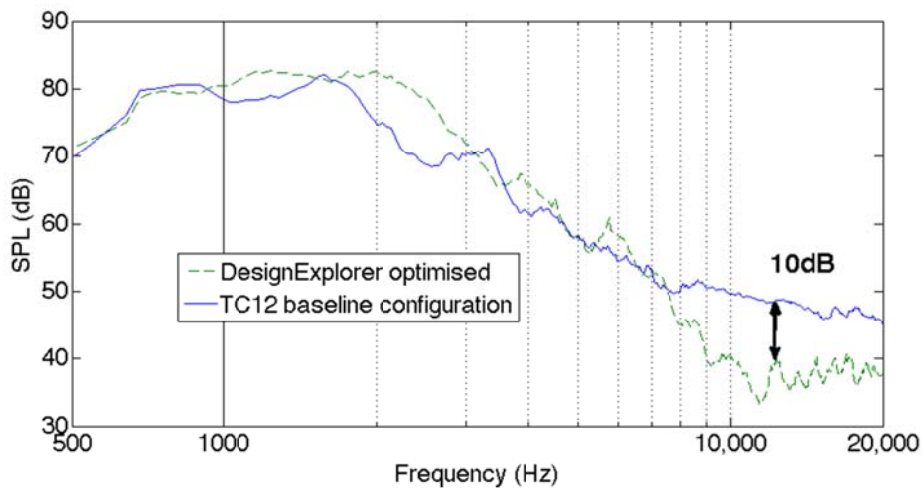

Fig. 16 Filtered sound spectrum for the optimised against he baseline at 8.09 degrees angle of attack

then the acoustic solver is turned on for an additional 1 000 timesteps. The timestep size is 2.5e-5s.

Directivity plots of the two concepts compared to eachother are shown in Fig. 14. As directivity is a measure of where sound is radiated from this shows that the new concept has no major effects on the locations from where sound is radiated. The mechanism of airfoil noise is generally dipole in nature and this is seen in the figure.

The vorticity contours of the DesignXplorer optimised concept and the baseline are overlayed onto eachother as seen in Fig. 15. The black regions in this diagram show areas where there is a major difference in vorticity between the two simulations. The major observation here is that the shear layer high vortical region (>1 000/s) is minimised by the effect of the novel concept on the flow field.

Fig. 16 compares the filtered acoustic data of the baseline to that of the DesignXplorer optimised solution. The data is also filtered using the Savitzky-Golay filter in MATLAB. Compared to the baseline solution the acoustic signals for this simulation appear to be noisier at frequencies beyond 1 000 Hz. Data in the mid-frequency range provides similar trends in results between the two configurations. From 6 000 to 20 000 Hz the DesignXplorer optimised solution appears to decrease the sound pressure level of the concept by about 10 dB.

By implementing the flap extension on the high lift device the flow field at the trailing edge was modified. This modification brings some stability to the shear layer within the spoiler cove, as shown by a decreased area of highly vortical flow within the cove. The additional flow stability in this region led to a decrease of high frequency noise of approximately 10 dB.

7. Conclusions

A novel concept for a high lift device is investigated, by means of computational studies, to increase aerodynamic performance and decrease aerodynamically generated noise of the TC12 profile in high lift configuration.

The zero order approach used a simplified method to optimise the TC12 profile flap in isolation of the rest of the high lift system. This optimisation showed a proof of concept that the suggested that the flap extension concept did increase aerodynamic performance of the flap airfoil in isolation. The optimisation process was successful on a system level. The geometric impingement of the flap extension on the flow field showed that, in the vicinity of the spoiler cove, the Coanda effect caused decreases in pressure at the recirculation region, and, at the flap extension, providing decreased lift from the overall high lift system. Premature stall was observed.

Using ANSYS DesignXplorer a different optimisation method was used to increase aerodynamic performance of the TC12 profile in high lift configuration. Due to limitations in computing time the results of the simulation were not converged but showed a trend towards convergence. The optimised results of this method showed better performance than that of the zero order optimisation routine solutions.

Acoustic simulations were performed on the baseline and DesignXplorer optimised solutions. Results of the acoustic simulations were found using the transient DES turbulence model. The Sound Pressure Level response of the DesignXplorer optimised concept was compared to the TC12 profile in high lift configuration. The simulations showed that the optimised solution caused a reduction in higher frequency tones of up to 10dB. This figure is of major relevance as the FP-7 framework calls for a reduction of noise of 10dB by the year 2020. The reduction of noise is due to the impingement of the flap concept on the flow field at the spoiler cove, which stabilises the fluctuating shear layer, thus reducing noise in this vicinity. This result shows that there is scope for further investigation of the concept as a noise reduction device.

References

Rudolph, K.C. (1996a), High-Lift Systems on Commercial Subsonic Airliners, NASA CR 4746, September.

Meredith, P. (1993), Viscous phenomena affecting high-lift systems and suggestions for future cfd development, AGARD CP-515.

Herr, M. (2012), Efficient and Airworthy Passive and Active Airframe Noise Control Strategies, VKI Lecture Airframe Noise Reduction.

Dobrzynski, W., Ewert, R., Pott-Pollenske, M., Herr, M. and Delfs, J. (2008), "Research at the DLR towards airframe noise prediction and reduction", *Aerospace Sci. Tech.*, **12**, 80-90

Zhang, X. (2010), "Airframe noise: High lift device noise", *Encyclopedia Aerospace Eng.*, DOI: 10.1002/9780470686652.eae338.

Casalino, D., Diozzi, F., Sannino, R. and Paonessa, A. (2008), "Aircraft noise reduction technologies: A bibliographic review", *Aerospace Sci. Tech.*, **12**, 1-17.

Busquin, P. (2001), European Aeronautics: a vision for 2020: meeting society's needs and winning global leadership, Luxembourg, European Commission.

Chen, H., Zhang, Y., Zhang, W. and Fu, S. (2012), "GA optimization design of multi- element airfoil", *Seventh International Conference on Computational Fluid Dynamics (IC- CFD7)*, 1-6.

Soulat, L., Dridi, W., Moreau, S. and Fosso-Pouangue, A. (2012), "Multi-objective optimization of a high-lift airfoil", *28th International Congress Of The Aeronautical Sciences.*

Taylor, P., Carrese, R., Winarto, H., Li, X., Sóbester, A. and Ebenezer, S. (2012), "A comprehensive preference-based optimization framework with application to high-lift aerodynamic design", *Eng. Optim.*, **44**(10), 1209-1227

Wild, J. (2008), "Multi-objective con- strained optimisation in aerodynamic design of high-lift systems", *Int. J. Comput. Fluid Dyn.*, **22**(3), 153-168.

Bizzarrini, N., Grasso, F. and Coiro, D. P. (2011), "Numerical Optimization for High Efficiency, Low Noise Airfoils", *29th AIAA Applied Aerodynamics Conference*, Honolulu, HI, USA, June.

Kuo, B.C. and Sarigul-Klijn, N. (2012), "Conceptual study of micro-tab device in airframe noise reduction: (ii) 3d computation", *Aerospace Sci. Tech.*, **17**(1), 32-39.

Modification de la forme dun profil (1980), ENSICA Lecture Notes ExperimatalAero, University Lecture.

Fullmer, J. (1947), "Two-dimensional wind-tunnel investigation of the naca 64 1-012 airfoil equipped with two types of leading-edge flap", Technical Report 1277, National Advisory Council for Aeronautics.

Drela, M. (2007), *XFOIL Subsonic Airfoil Development System User Guide*.

Brezillon, J., Dwight, R. and Wild, J. (2008), "Numerical aerodynamic optimisation of 3D high-lift configurations", *26th International Congress Of The Aeronautical Sciences*.

Ffowcs-Williams, J.E. and Hawking, D.L. (1969), "Sound generation by turbulence and surfaces in arbitrary motion", *Phil. Tran. Royal Soc. London A*, **342**, 264-321.

EC